Electronic Supplementary Material (ESI) for CrystEngComm.

Electronic Supplementary Information

Single Crystal-to-Single Crystal transformation induced by water-ammonia equilibrium changes

by Marek Daszkiewicz,[a] Mariola Puszyńska-Tuszkanow,[b] Zbigniew Staszak,[c] Ida Chojnacka,[b] Hanna Fałtynowicz,[b] Maria Cieślak-Golonka,[b]

[a] Institute of Low Temperature and Structure Research, Polish Academy of Sciences, Okólna 2, P.O. Box 1410, 50-950 Wrocław, Poland

[b] Faculty of Chemistry, Wrocław University of Technology, Wybrzeże Wyspiańskiego 27, 50-270 Wrocław, Poland

[c] Faculty of Computer Science and Management, Wrocław University of Technology, Wybrzeże Wyspiańskiego 27, 50-270 Wrocław, Poland

Experimental:

Preparation of $[Ni(mph)_2(NH_3)_2(H_2O)_2]\cdot 1.23NH_3$ (1) and $[Ni(mph)_2(NH_3)_2(H_2O)_2]\cdot 1.26H_2O$ (2).

Crystals of **(1)** were prepared as follows: 1 mmol (0.240 g) of $NiCl_2\cdot 6H_2O$ dissolved in 10 cm^3 of aqueous ammonia solution (25 %) was added to 2 mmol (0.360 g) of 5-methyl-5-phenylhydantoin dissolved in 10 cm^3 of aqueous ammonia (25 %). The resulting deep violet solution was allowed to evaporate at room temperature. After four days, violet crystals (**1**) of X-ray measurements quality were obtained. During next four days the violet crystals of (**1**) transforms completely into blue crystals of (**2**). At the same time the color of solution changed from dark violet to light blue. The blue crystals are stable at room temperature. The composition and structure of both complexes were determined by X-ray single crystal structure analysis, FT-IR spectra, TG analysis (TG/FTIR) and electronic spectra.

Elemental analysis calcd (%) for: $C_{20}H_{32.5}NiN_{7.5}O_6$ **(1)** (Mw = 528.12 g/mol): C, 45.34, H, 6.04, N, 19.41, and $C_{20}H_{30.5}NiN_6O_{7.5}$ (**2**) (Mw = 529.98 g/mol): C, 45.23, H, 5.78, N, 15.82. Found, respectively for (**1**): C, 45.37, H, 5.69, N, 18.80, and (**2**): C, 45.37, H, 5.30, N, 15.70.

Exposition of blue crystals (**2**) to the NH_3 atmosphere resulted in formation of violet microcrystalline powder (**1**). Air atmosphere triggers retransformation to the blue powder (**2**).

Physical measurements

Elemental analyses (carbon, hydrogen, and nitrogen) were performed with a Perkin-Elmer 240C elemental analyzer.

Structural research

X-ray crystallography: X-ray diffraction data for the studied compounds were collected on an Oxford Diffraction four-circle single crystal diffractometer equipped with a CCD detector and using graphite-monochromated MoKα radiation (λ=0.71073 Å). The crystal structures were solved by direct methods and refined by a full-matrix least-squares method using the SHELXL-2014 program [S1]. The results are presented in Tables S1 – S5.

Table S1. Crystal data and structure refinement parameters for organic ligand (mph), $[Ni(mph)_2(NH_3)_2(H_2O)_2]\cdot 1.23NH_3$ (**1**) and $[Ni(mph)_2(NH_3)_2(H_2O)_2]\cdot 1.26H_2O$ (**2**). For all: T [K] 295(2), λ [Å] 0.71073,

	mph	1	2
Crystal data			
Chemical formula	$C_{10}H_{10}N_2O_2$	$C_{20}H_{28}N_6NiO_6\cdot 1.23(NH_3)$	$C_{20}H_{28}N_6NiO_6\cdot 1.26(H_2O)$
M_r	190.20	528.11	529.98
Crystal system, space group	Monoclinic, $P2_1$	Triclinic, P-1	Monoclinic, $P2_1/c$
a, b, c (Å)	7.3454 (13), 6.2161 (10), 10.7970 (18)	6.7306 (12), 8.9921 (13), 10.4338 (15)	10.3679 (10), 6.4569 (7), 18.3125 (15)
α, β, γ (°)	90, 108.144 (15), 90	95.898 (12), 91.502 (13), 99.545 (14)	90, 98.023 (7), 90
V (Å^3)	468.48 (14)	618.84 (17)	1213.9 (2)
Z	2	1	2
μ (mm^{-1})	0.10	0.83	0.85
Crystal size (mm)	0.41 × 0.22 × 0.15	0.35 × 0.27 × 0.25	0.23 × 0.20 × 0.18
Data collection			
Absorption correction	–	Numerical	Numerical
T_{min}, T_{max}	–	0.824, 0.899	0.837, 0.906
No. of measured, independent and observed [$I > 2\sigma(I)$] reflections	6586, 2123, 1386	7749, 2611, 2107	15944, 2684, 1918
R_{int}	0.074	0.069	0.062
(sin θ/λ)$_{max}$ (Å^{-1})	0.649	0.633	0.641
Refinement			
$R[F^2 > 2\sigma(F^2)]$, $wR(F^2)$, S	0.067, 0.198, 1.00	0.056, 0.151, 1.11	0.052, 0.153, 1.08
No. of reflections	2123	2611	2684
No. of parameters	129	163	163
No. of restraints	1	0	0
$\Delta\rho_{max}$, $\Delta\rho_{min}$ (e Å^{-3})	0.27, -0.22	0.45, -0.54	0.84, -0.44
Absolute structure	Refined as a perfect inversion twin.	–	–
Absolute structure parameter	0.5	–	–

Table S2. Selected bond lengths [Å] and angles [°] for organic ligand (**mph**).

Bond lengths [Å]	**(mph)**	Angles [°]	**(mph)**
C(2)=O(2)	1.215	O(2)-C(2)-N(1)	128.4
C(4)=O(4)	1.213	O(2)-C(2)-N(3)	124.5
N(1)-H	0.860	O(4)-C(4)-C(5)	125.8
N(3)-H	0.860	O(4)-C(4)-N(3)	126.9
N(1)-C(2)	1.320	-	-
C(2)-N(3)	1.405	-	-
N(3)-C(4)	1.349	-	-

Table S3. Selected bond lengths [Å] and angles [°] for $[Ni(mph)_2(NH_3)_2(H_2O)_2]\cdot 1.23NH_3$ (**1**) and $[Ni(mph)_2(NH_3)_2(H_2O)_2]\cdot 1.26H_2O$ (**2**).

Bond lengths [Å]	**(1)**	**(2)**	Angles [°]	**(1)**	**(2)**
Ni-O(1)W#1	2.085(3)	2.106(3)	O(1)W#1-Ni-O(1)W	180.0	180.0
Ni-O(1)W	2.085(3)	2.106(3)	O(1)W#1-Ni-N(4)	91.9(2)	92.9(2)
Ni-N(4)	2.100(3)	2.088(3)	O(1)W-Ni-N(4)	88.1(2)	87.2(2)
Ni-N(4)#1	2.100(3)	2.088(3)	O(1)W#1-Ni-N(4)#1	88.1(2)	87.2(2)
Ni-N(3)	2.179(2)	2.133(2)	O(1)W-Ni-N(4)#1	91.9(2)	92.9(2)
Ni-N(3)#1	2.179(2)	2.133(2)	N(4)-Ni-N(4)#1	180.0	180.0
N(1)-C(2)	1.353(3)	1.351(4)	O(1)W#1-Ni-N(3)	89.5(1)	89.2 (2)
N(1)-C(5)	1.445(4)	1.441(4)	O(1)W-Ni-N(3)	90.5(1)	90.8(2)
N(1)-H(1)	0.860	0.860	N(3)-Ni-N(3)#1	180.0	180.0
C(2)-O(2)	1.235(4)	1.229(4)	-	-	-
C(2)-N(3)	1.393(4)	1.396(3)	-	-	-
N(3)-C(4)	1.335(4)	1.329(4)	-	-	-
C(4)-O(4)	1.230(4)	1.247(4)	-	-	-
C(4)-C(5)	1.546(4)	1.546(4)	-	-	-
C(5)-C(21)	1.519(4)	1.527(5)	-	-	-
C(5)-C(11)	1.526(5)	1.518(4)	-	-	-

Symmetry code: #1 -x,-y,-z+1

Table S4. Hydrogen bonds geometry in organic ligand (**mph**) [Å and °].

(**mph**)

D-H...A	d(H...A)	d(D...A)	<(DHA)
N(3) – H(3)…O(2)^{ii}	1.98	2.786(5)	156.6
N(1) – H(1)…O(4)^{i}	2.00	2.861(5)	173.5

Symmetry codes: #i x, y-1, z; #ii -x, y+1/2, -z+1

Table S5. Hydrogen bonds geometry in [Ni(mph)$_2$(NH$_3$)$_2$(H$_2$O)$_2$]·1.23NH$_3$ (**1**) and [Ni(mph)$_2$(NH$_3$)$_2$(H$_2$O)$_2$]·1.26H$_2$O (**2**) [Å and °].

(1)

D-H...A	d(H...A)	d(D...A)	<(DHA)
N(1)-H(1)...O(2)#2	2.12	2.976(3)	174.7
O(1)W-H1W1...O(4)	1.89	2.708(3)	146.7
O(1)W-H2W1...O(2)#1	1.94	2.739(3)	144.2
O(2)W-H1W2...O(4)#3	1.93	2.776(6)	153.0
O(2)W-H2W2...O(4)	2.24	2.994(6)	140.7
N(1A)-H1A1...O(2)W	2.33	3.156(9)	154.9

Symmetry codes: #1 -x+1,-y,-z #2 -x,-y,-z #3 -x+1,y-1/2,-z+1/2

(2)

D-H...A	d(H...A)	d(D...A)	<(DHA)
N(1)-H(1)...O(2)#2	2.10	2.953(3)	174.7
O(1)W-H1W1...O(4)	2.08	2.889(4)	146.5
O(1)W-H2W1...O(2)#1	2.17	2.951(4)	143.8

Symmetry codes: #1 -x,-y,-z+1 #2 -x,-y,-z+2 #3 x,y-1,z #4 x+1,y+1,z

Spectroscopic studies

Infrared spectra of both the complexes and the organic ligand were recorded as pellets (4000–400 cm^{-1}) and Nujol mulls (600–100 cm^{-1}) using Perkin–Elmer1600 and Perkin–Elmer FTIR 2000 spectrophotometers, respectively (Table S6).

Table S6. Selected IR bands (cm^{-1}) for 5-methyl-5-phenylhydantoin (mph) and its complexes: $[Ni(mph)_2(NH_3)_2(H_2O)_2]\cdot 1.23NH_3$ **(1)** and $[Ni(mph)_2(NH_3)_2(H_2O)_2]\cdot 1.26H_2O$ **(2)**.

(mph)	(1)	(2)	Assignment
-	3550_{w}	3604_{w}	ν(O-H) / $\nu(N\text{-}H)_{NH3}$
	3354_{w}	3382_{w}	
	3230_{s}	3240_{s}	
3280_{s}			ν(N(1)-H)
3206_{s}			ν(N(3)-H)
2987_{w}	2988_{w}	2988_{w}	ν(C-H)
2937_{w}	2941_{w}		
1769_{m}	1720_{w}	1720_{w}	ν(C(2)=O)
1725_{w}	1687_{s}	1686_{s}	ν(C(4)=O)
1716_{s}			
-	1614_{bs}	1621_{bs}	δ (H_2O)/
	$\sim 1600_{sh}$	$\sim 1600_{sh}$	δ (H-N-H)
1431_{w}	-	-	δ(N(3)-H)
1365_{s}	1364_{m}	1364_{m}	δ(N(1)-H)
-	-	701_{bs}	ρ_r (H_2O)
	585_{bw} 456_{m}	603_{bw} 474_{m}	ρ_w (H_2O)
-	527_{m}	509_{m}	ν ($Ni\text{-}N_{NH3}$)
	347_{m} 307_{m}	348_{m} 311_{m}	ν ($Ni\text{-}O_{H2O}$)
-	226_{m}	203_{m}	$\nu(Ni\text{-}N_L)$

s- strong, m- medium, ov- overlaping, w- weak, vw- very weak

The electronic spectra (5000 - 50000 cm^{-1}) were measured on a Cary 500 Scan UV–Vis-NIR Spectrophotometer (Varian) in diffuse reflectance (Fig. S1).

In order to obtain accurate values of the band positions, the spectra were analyzed using variable digital filter method [S2-S7] with the following filter parameters: number determining the degree of resolution enhancement, a = 200; the integer number determining the filter width, N = 20; the increment between points (step) = 50 cm^{-1}. As the bands are slightly asymmetric (Fig. S1) we have made the calculations of the crystal field (CF) and B parameters assuming both O_h - D_q and lower tetragonal D_{4h} (D_q, D_s, D_t) symmetries. (Tables S7 and S8). These calculations were based on the Tanabe-Sugano diagrams and Perumareddi matrices (without spin–orbit coupling parameter) for spin allowed transitions [S8-S10].

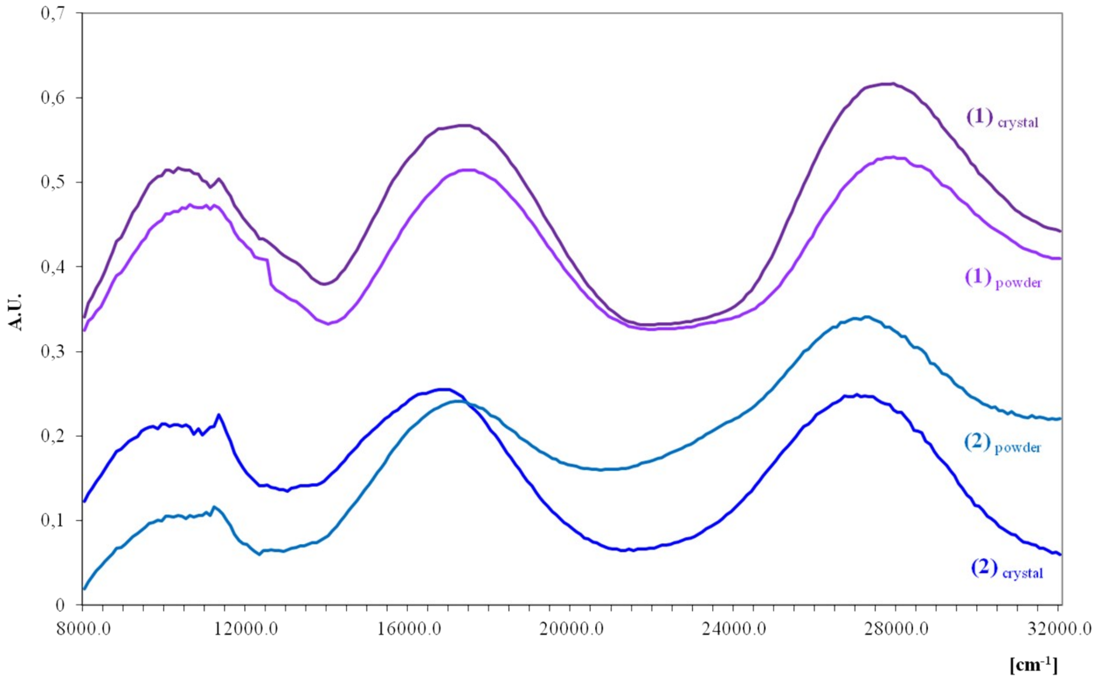

Fig. S1. Diffuse reflectance spectra of **(1)** and **(2)** complexes.

The bands have been attributed to the d-d spin-allowed transitions in the Ni(II) ion (d^8). The transitions are from the ground state $^3A_{2g}(^3F)$ to the $^3T_{2g}(^3F)$, $^3T_{1g}(^3F)$ and $^3T_{2g}(^3P)$ excited states, respectively, with some splitting under symmetry lowering. Table S7 shows that the values of CF parameters calculated assuming O_h symmetry changes systematically from NiN_6 to NiO_6. The slight change between **(1)** and **(2)** confirms the identity of their first coordination sphere. However, it shows also some influences of the second coordination sphere and its importance on the direct metal ion surroundings. The values of CF and Racah B parameters of the respective crystal and powder are comparable confirming their chemical identity. Unexpectedly enough, the slight differences in the band positions and CF parameters between (**1**) and (**2**) are sufficient enough to change the color of the species what can be important in potential application as sensors. Particularly, it can be valid for compound **(2)** due to its greater stability than **(1)**.

Table S7. Crystal field and Racah B parameters for $[Ni(mph)_2(NH_3)_2(H_2O)_2]\cdot 1.23NH_3$ **(1)** and $[Ni(mph)_2(NH_3)_2(H_2O)_2]\cdot 1.26H_2O$ **(2)** (cm^{-1}) in O_h symmetry. Simple aqua- and ammina Ni(II) complexes were included, for comparison.

	$Ni(NH_3)_6^{2+}$[S10]	(1) crystal	(1) powder	(2) crystal	(2) powder	**$Ni(H_2O)_6^{2+}$**[S10]
D_q	**1075**	**1067**	**1077**	**1037**	**1059**	**850**
B	**881**	**851**	**857**	**842**	**838**	**930**

More detailed analysis of the spectra revealed lower than O_h symmetry (Table S8 and Scheme S1).

Table S8. The assignment for the bands in the Ni(II) ion in **(1)** and **(2)** (in cm^{-1}) and crystal field and Racah B parameters for D_{4h} symmetry**.**

$\mathbf{O_h}$	**(1)**	**(2)**	$\mathbf{D_{4h}}$	**(1)**	**(2)**
$^{3}\mathrm{T}_{2g}(^{3}\mathrm{F})$	10450	10150	$^{3}\mathrm{E}_{g}$	9950	9500
			$^{3}\mathrm{B}_{2g}$	11450	11600
$^{1}E_{g}$	~12400	~12500	$^{1}A_{1g}$ $^{1}B_{1g}$	13000	
$^{3}\mathrm{T}_{1g}(^{3}\mathrm{F})$	17300	16850	$^{3}\mathrm{A}_{2g}$	16700	15600
			$^{3}\mathrm{E}_{g}$	17900	17100
$^{1}T_{2g}$	~22900	~22300	$^{1}E_{g}$ $^{1}B_{2g}$	22700	
$^{3}\mathrm{T}_{2g}(^{3}\mathrm{P})$	27650	27050	$^{3}\mathrm{A}_{2g}$	27200	22200
			$^{3}\mathrm{E}_{g}$	28200	23000

CF and Racah B parameters

$\mathbf{D_{4h}}$	**(1)**	**(2)**
Dq	1147	1161
B	849	842
Dt	-327	-327
Ds	-208	-153

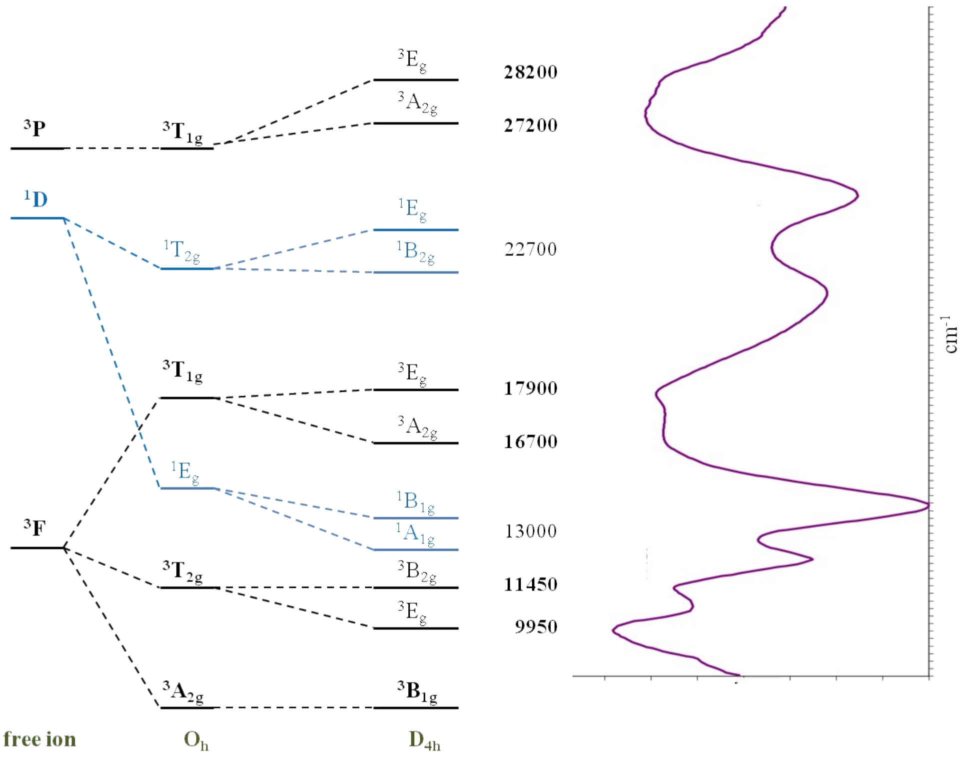

Scheme S1. Correlation between the Tanabe-Sugano diagram (d^8 configuration) for O_h and D_{4h} symmetries and the effect of filtration for the spectrum of crystal (**1**).

The values of the magnetic moment obtained for the nickel(II) complexes **(1)** and **(2)** are 2.84 μ_B and 2.86 μ_B. These values are slightly lower than those usually observed for nickel(II) octahedral complexes (μ_{eff} 2.90, μ_{so} 2.83). The lowering of μ values can be attributed to the real symmetry of **(1)** and **(2)** which are lower than O_h.

Thermogravimetric (TG) and differential thermal analysis

DTA measurements were carried out in Laboratory of Thermal Analysis and Calorimetry at Wroclaw University of Technology. Modular high-temperature differential scanning calorimeter Line 96 SETARAM was used to investigate both phase equilibria and mass changes in the samples, simultaneously. Moreover, Line 96 associated with FTIR spectrometer (Tensor 27, Bruker) was used for registration and identification of gaseous reaction products. Decomposition of the samples was carried out in the platinum crucibles. Measurements were conducted in the temperature range between 20-500 °C with heating rate 5 °C/min. Argon (99.9999 % purity) was used as protective gas as well as carrier gas. FTIR spectra were recorded with resolution of 2 cm^{-1} in the 7 000 - 420 cm^{-1} range.

References

S1. G.M. Sheldrick, *Acta Cryst.*, 2008, **A64**, 112
S2. G. Bierman and H. Ziegler, *Anal. Chem.*, 1986, **58**, 536.;
S3. J. Myrczek, *Spectrosc. Lett.*, 1990, **23**, 1027.;
S4. M. Cieślak-Golanka, M. Raczko and Z. Staszak, *Polyhedron*, 1992, **11**, 2549.;
S5. W. Bronowska, Z. Staszak, M. Daszkiewicz, M. Cieślak-Golonka and A. Wojciechowska, *Polyhedron*, 2002, **21**, 997;

S6. M. Daszkiewicz, Z. Staszak, A. Pietraszko, W. Bronowska and M. Cieślak-Golonka, *Struct. Chem.*, 2006, 17, 599; A. Bartecki, Z. Staszak, *Comp. Enh. Spectrosc.*, 1984, **2**, 129.;
S7. D. Miernik, A. Arkowska, E. Grażyńska and Z. Staszak, *Spectrosc. Lett.*, 1991, **24**, 371.
S8. J.R. Perumareddi, *J. Phys. Chem.*, 1972, **76**, 3401.;
S9. J.S. Merriam and J.R. Perumareddi, *J. Phys. Chem.*, 1975, **79**, 142.;
S10. A.B.P. Lever, Inorganic Electronic Spectroscopy, second ed., Elsevier, New York, 1984.